Available online at www.sciencedirect.com
ScienceDirect
Energy Conversion and Management xxx (2008) xxx–xxx
ENERGY CONVERSION & MANAGEMENT
www.elsevier.com/locate/enconman

Experimental study on improved two-bed silica gel–water adsorption chiller

Zaizhong Xia [a,*], Dechang Wang [b], Jincui Zhang [b]

[a] Institute of Refrigeration and Cryogenics, Shanghai Jiao Tong University, Shanghai 200030, PR China
[b] College of Electromechanical Engineering, Qingdao University, Qingdao 266071, PR China

Received 14 September 2006; received in revised form 5 May 2007; accepted 22 December 2007

Abstract

A novel silica gel–water adsorption chiller with two chambers has been built in Shanghai Jiao Tong University (SJTU). This chiller combines two single bed systems (basic system) without any vacuum valves. One adsorber, one condenser and one evaporator are housed in the same chamber to constitute one adsorption/desorption unit. In this work, the chiller is developed and improved. The improved chiller is composed of three vacuum chambers: two adsorption/desorption vacuum chambers (the same structure as the former chiller) and one heat pipe working vacuum chamber. The evaporators of these two adsorption/desorption units are combined by a heat pipe. So, no valves are installed in the chilled water sub system and one vacuum valve connects the two adsorption/desorption chambers together to improve its performance. The performance of the chiller is tested. As the results, the refrigerating capacity and the COP of the chiller are, respectively, 8.69 kW and 0.388 for the heat source temperature of 82.5 °C, the cooling water temperature of 30.4 °C and the chilled water outlet temperature of 11.9 °C. For a chilled water outlet temperature of 16.5 °C, the COP reaches 0.432, while the refrigerating capacity is near 11 kW. There is an improvement of at least 12% for the COP compared with the former chillers.

Keywords: Adsorption chiller; Silica gel–water; Experiments; Vacuum chamber

1. Introduction

An adsorption cooling system has a potential to replace CFCs of HCFCs existing in traditional compression refrigeration. No crystallization and corrosion problem is another competitive merit compared with an absorption cooling system. Therefore, adsorption refrigeration has attracted much attention in recent decades.

Many efforts have been made to improve the system performance. To improve the COP (coefficient of performance) value, Shelton [1] and Critoph [2], respectively, introduced two advanced adsorption cycles: a thermal wave cycle and a convection thermal wave cycle. According to Pons [3], the zeolite–water adsorption cooling system had a 40–120 W kg^{-1} SCP (specific cooling power) and a 0.3–0.4 COP when it worked in the thermal wave cycle in the air conditioning mode. From Sward's results [4], the cycle COP was higher than 1.2 for a thermal-wave adsorption heat pump cycle. Critoph [5,6] studied the convection thermal wave cycle with a packed bed of inert material. His experimental heat transfer measurements and cycle simulations showed that a COP of 0.90 was obtained for a specific carbon when evaporating at 5 °C and condensing at 40 °C with a generating temperature of 200 °C. The modest system regenerator effectiveness has been 0.8. These results indicated the high feasibility of those two adsorption cycles, though there are some difficulties to putting them into practice. As a similar effect, a mass recovery process was introduced to an adsorption system. Wang's study results [7] showed that 10–20% improvement of COP was obtained with a mass recovery process. To improve the system performance under a low temperature driving heat

* Corresponding author. Tel.: +86 021 3420 6296; fax: +86 021 3420 6548.
E-mail address: xzz@sjtu.edu.cn (Z.Z. Xia).

0196-8904/$ - see front matter © 2008 Elsevier Ltd. All rights reserved.
doi:10.1016/j.enconman.2007.12.019

Nomenclature

COP	coefficient of performance	*Subscripts*	
$C_{p,w}$	specific heat of water, kJ kg^{-1} °C^{-1}	e	evaporator
C_{cu}	specific heat of cuprum, kJ kg^{-1} °C^{-1}	*h*	heat, hot
$\dot{G}$	mass flow rate, kg s^{-1}	in	inlet
L	latent heat of methanol, kJ kg^{-1}	meth	methanol
m	total mass of adsorbent in chiller, kg	me	methanol evaporator
n	times of data acquisition in one cycle	out	outlet
Q	heat power, kW	ref	refrigeration
SCP	specific cooling power, kW/kg adsorbent	we	water evaporator
T	temperature, °C	*Superscript*	
τ	time, s	*i*	order number of data acquisition interval

source, Saha et al. [8,9] proposed a multi-bed, dual mode silica gel–water adsorption chiller to utilize effectively solar energy or a waste heat source of temperature between 40 and 95 °C. This work is very valuable for energy utilization, though the performance is quite low.

Poor mass and heat recovery is the main factor to forbid industrialization and commercialization of an adsorption cooling system. Many researches have been attempted to improve the mass and heat transfer of the system. Eun et al. [10,11] used the silica gel/expanded graphite composite blocks to enhance the heat and mass transfer to improve the performance of the cooling systems. Miltkau and Dawoud [12] recommended that the zeolite layer thickness must not exceed 2.5 mm in order to obtain good heat and mass transfer performance. Tatlıer et al. [13] attempted to use zeolite synthesized as a continuous thin layer on the heat exchanger tubes to enhance the heat and mass transfer.

In the field of solar energy and waste heat utilization, an adsorption chiller would be a competitive choice. In all the optional adsorption systems for low temperature heat source utilization, the silica gel–water adsorption system is one of most favorable and available systems. Many efforts have been made to improve the system performance and industrialize it in this field. Saha, Chua, Kashiwagi, Akisawa et al. [8,9,14–18,20] have gone deep into the study of the silica gel–water adsorption system, especially in the field of low temperature waste heat utilization. Based on their efforts, the two adsorber, silica gel–water adsorption system has been commercialized in a small scale in Japan [8], but the four vacuum valves inserted inside the chiller were difficult to replace when troubles occurred. Furthermore, such valves, with a large vapor flow cross section, were difficult to manufacture and a highly technical process is necessary.

At SJTU, a continuous silica gel–water adsorption chiller has been exploited [19] based on the work mentioned above. This chiller had a COP over 0.5 and a refrigerating capacity of 9 kW at 80 °C heat source temperature, 13 °C evaporating temperature and 25 °C cooling temperature. There were no vacuum valves installed in the chiller. So, the vacuum leakage problem and pressure drop caused by the vacuum valves were absolutely avoided. The operating reliability of the system was greatly improved. However, a water tank and four electric valves were indispensable to help the system finish the mass recovery like process (heat recovery process between two evaporators). Thus, the complexity of the system and the number of moving parts increased so that commercialization of this kind of chiller has been impacted, though its performance is satisfying.

In this study, one improved silica gel–water adsorption chiller is developed and employed based on our former primary work [19,21]. In this improved chiller, one condenser, one adsorber and one evaporator are housed in one chamber to constitute an adsorption/desorption unit similar to the one designed in [19]. Two such units are combined in evaporators by a heat pipe that can insulate the heat transfer between the two evaporators. Only one vacuum valve is installed between the two units outside the chiller to fulfill the mass recovery process instead of the mass recovery like process that is not effective enough to improve the performance. The water tank and electric valves in the chilled water system are spared. Then, the reliability of the system rises. The results of the experiments indicate that such adsorption chiller is very effective to use with a 60–85 °C heat source, and the performance of the system is improved greatly compared with the former chillers. Based on the achievements, more than 10 chillers have been manufactured successfully to be driven by solar energy and waste heat from an engine.

2. System description

2.1. Prototype

The schematic diagram of the improved silica gel–water adsorption chiller is shown in Fig. 1, and the photograph is shown in Fig. 2. This chiller combines three vacuum chambers. One adsorber, one condenser and one evaporator are housed in the same chamber as one adsorption/desorption

Please cite this article in press as: Xia ZZ et al., Experimental study on improved two-bed ..., Energ Convers Manage (2008), doi:10.1016/j.enconman.2007.12.019

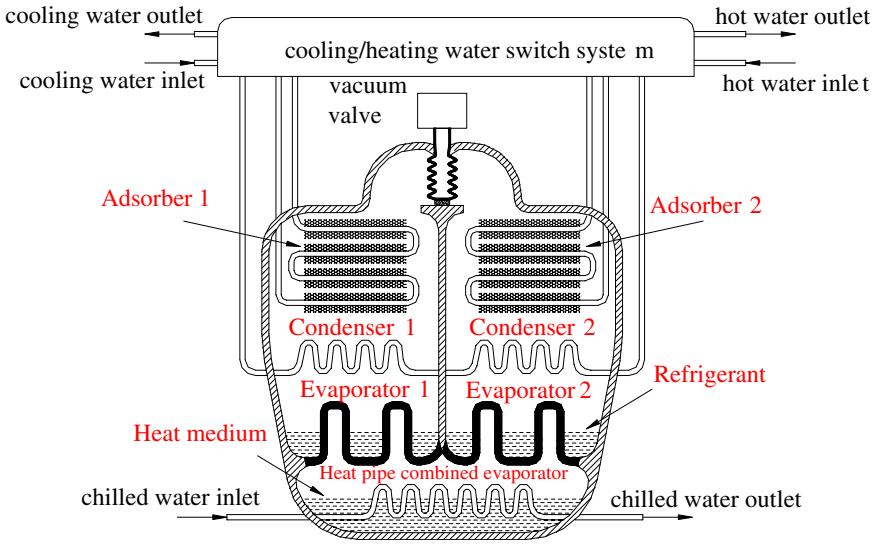

Fig. 1. Schematic diagram of the improved silica gel–water adsorption chiller.

Fig. 2. Photograph of the improved silica gel–water adsorption chiller.

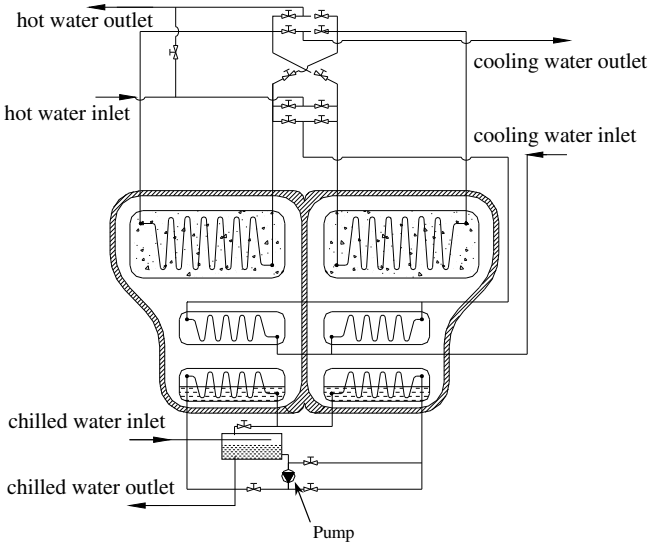

Fig. 3. The former silica gel–water adsorption chiller [19].

unit. The two adsorption/desorption units are combined in the evaporators by a heat pipe heat exchanger into one integrated continuous adsorption chiller. The evaporators are alternately heated by the chilled water through a gravity heat pipe that effectively isolates the heat exchange between the two evaporators. The cooling/heating water switch system is composed of 11 electric valves, the same as the former system as shown in Fig. 3. One vacuum valve is installed between the two chambers for the mass recovery process. The refrigerant is water and the heat pipe working media is methanol.

The adsorber is one compact tube fin heat exchanger. The thickness of the silica gel layer filled between two fins inside the adsorber is 2.5 mm and the length from the heat transfer tube to the mass transfer channels is less than 12 mm. The micro-pored silica gel with 0.50–1 mm diameter is filled between two aluminum fins with a 2.5 mm space that is as thick as the silica gel layer. In the adsorbent side, the heat transfer area of each adsorber is 3.3 m^2 for the copper heat transfer tubes and 60.6 m^2 for the fins. Each adsorber contains 52 kg silica gel.

The condensers are tube shell whose shell is also the chamber shell. They are connected to each other in series, different from our former system. The cooling water flows into one condenser first and then into the other, last into the adsorber through the cooling/heating water switch system. The condensing area is 2.8 m^2 for each condenser.

The two evaporators are combined together by a heat pipe (HP). Both the hot end and the cold end of the HP are tube shell. The exterior surface of the copper tubes in

Please cite this article in press as: Xia ZZ et al., Experimental study on improved two-bed ..., Energ Convers Manage (2008), doi:10.1016/j.enconman.2007.12.019

the upside (cold end, water evaporators) of the HP is a water evaporating surface that is covered by porous layer to enhance the heat transfer, and the internal surface is the methanol condensing surface. The methanol will evaporate on the exterior surface of the heat exchange tubes in the bottom (hot end, methanol evaporator) of the HP and condense on the internal surface of the tubes in the upside of one evaporator Simultaneously, the other evaporator is heated by the condensate, so its temperature is higher than that of the working evaporator and the hot end of the HP. As a result, the heat exchange of the idle evaporator is isolated from the working evaporator and the hot end of the HP. In the methanol working cycle, the methanol vapor evaporates from the hot end of the HP and flows into the tubes in the cold end from one end, then, returns to the hot end of the HP from the other end after being condensed. A loop is formed for the methanol flow; thereby, the evaporator is a loop heat pipe. In this paper, Evaporator 1 or Evaporator 2 is termed the Water Evaporator, and the hot end of the heat pipe is termed the Methanol Evaporator.

The structure of the chiller causes one evaporator and one condenser to be idle anytime so as to decrease the utilization ratio of the evaporators and the condensers, but four vacuum valves for the switch between the adsorption and desorption processes are removed. The vacuum leakage and the complexity of the system are absolutely avoided as well as the former chiller, and the improved HP evaporator has spared four electric valves and decreased the heat loss compared with the former system. Therefore, the reliability of the chiller is improved highly; and meanwhile, the performance of the chiller is also increased greatly.

2.2. Improvement in the structure

The most important improvement for the improved chiller is in the structure of the evaporator. Compared with the evaporator of the former chiller shown in Fig. 3, all the valves, one pump and one chilled water tank are removed in the chilled water circuit. In the former chiller, the pump in the internal loop of the chilled water (loop between evaporator and chilled water tank) will consume much electric energy because the pressure drop of the plate fin evaporator is much higher than that of a tube shell evaporator. Moreover, much refrigerating capacity loss results from the evaporator for the residual chilled water with a low temperature in the evaporator just after the desorption process causes more refrigerant vapor to condense in the evaporator. Therefore the evaporator in the improved chiller is simpler, more efficient and more reliable.

The installation of a mass recovery vacuum valve is the second important improvement for the improved chiller. The effect of the mass recovery process will be enhanced rather than the mass recovery like process, especially when the chiller is driven by a heat source with temperature lower than 65 °C.

2.3. Working principle

The cycle process of this chiller is similar to the former system shown in Fig. 3. Fig. 4 shows the ideal cycle processes of the improved chiller and the former chiller, where the process $A \rightarrow B \rightarrow C \rightarrow D \rightarrow E \rightarrow F \rightarrow A$ represents the improved chiller and the process $A' \rightarrow B \rightarrow C \rightarrow D' \rightarrow E \rightarrow F \rightarrow A'$ the former chiller. The real mass recovery process is more effective than the mass recovery like process. Therefore, at the end of the mass recovery process, the adsorber will desorb or adsorb more refrigerant for the improved chiller than for the former chiller. The cyclic adsorption capacity of the adsorber is augmented. It must be pointed out that the real mass recovery process is quite necessary if the heat source temperature is quite low because the small temperature lift for the adsorber causes a quite small cyclic adsorption capacity.

Working through one whole cycle, the chiller must finish six different phases: desorption process in adsorber 1 and adsorption process in adsorber 2, mass recovery process from adsorber 1 to adsorber 2, heat recovery process from adsorber 1 to adsorber 2, adsorption process in a desorber 1 and desorption process in adsorber 2, mass recovery process from adsorber 2 to adsorber 1 and heat recovery process from adsorber 2 to adsorber 1. Because some phases are similar to each other on principle, these six phases can be summarized into three processes: adsorption/desorption process, mass recovery process and heat recovery process.

2.3.1. Adsorption/desorption process

The cooling water is switched into one adsorber by the cooling/heating water switch system, and then, the adsorber is cooled to adsorb. At the same time, hot water flows into the other adsorber, and then, the adsorber is heated to desorb. The adsorption and desorption process are, respectively, shown as $E \rightarrow F$ and $B \rightarrow C$ ideally in Fig. 4. This process is the main phase of refrigeration output and regeneration for the chiller.

2.3.2. Mass recovery process

When the adsorption/desorption process is nearly to the end, the vacuum valve is opened, and the mass recovery process is realized. In this process, the desorber continues

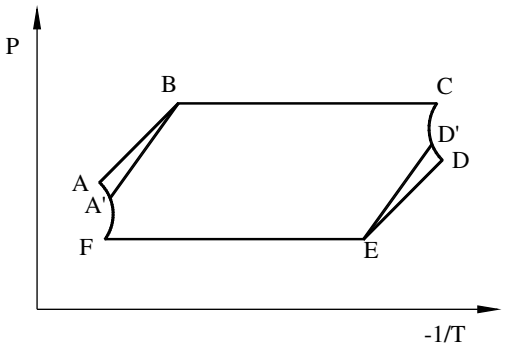

Fig. 4. Clapeyron diagram of ideal cycle.

Please cite this article in press as: Xia ZZ et al., Experimental study on improved two-bed ..., Energ Convers Manage (2008), doi:10.1016/j.enconman.2007.12.019

to be heated and the adsorber cooled. The refrigerant vapor from the desorber will be adsorbed by the adsorber. So, this process can be called "*secondary adsorption/desorption*". During this process, there isn't any refrigeration output. The desorber works from C to D and the adsorber from F to A.

2.3.3. Heat recovery process

At the end of the mass recovery process, the vacuum valve is closed and the hot water is bypassed. Then, the adsorber is connected with the desorber by the cooling/heating water switch system. Powered by the cooling water pump, the cooling water in the adsorber flows into the desorber, and the hot water in the desorber is pushed into the adsorber. The adsorber will change into the desorber and the desorber into the adsorber. When the hot water in the desorber completely flows into the adsorber, this process will be over, and a new adsorption/desorption process will begin.

3. Test system

Fig. 5 shows the experimental system of the improved chiller. Three water tanks are set in the heating water, the cooling water and the chilled water sub systems to keep their temperature changing smoothly. One flow meter is installed in each water system. Valves V2, V3 and V4 act as the controllers for the flow rates. The heat source is provided by a tube shell heat exchanger that is heated by 6 bar steam flow. The hot water temperature is controlled by valve V1. The chilled water and cooling water temperatures are, respectively, controlled by valves V5 and V7, and valves V6 and V8 are the assistant controllers. The chilled water tank has a higher position than the cooling water tank so that the superfluous chilled water can flow into the cooling water tank through the over flow pipe. The cooling water is discharged by another over flow pipe.

The water inlet and outlet temperatures of the chiller are measured by six PT100 platinum resistances, grade A. The water flow rates are measured by three flow meters. The data are acquired by a Keithly 2700 Multimeter/Data Acquisition System interfaced by a PC. A data acquisition programme reads and stores data about every 9 s.

The refrigerating power and heating power are calculated as follows:

Refrigerating capacity:

$$Q_{\mathrm{ref}} = \sum_{i=1}^{n} [\dot{G}_{\mathrm{chilled}} C_{\mathrm{p,w}} (T^{i}_{\mathrm{chilled,in}} - T^{i}_{\mathrm{chilled,out}})]/n, \tag{1}$$

and heating power:

$$Q_{\mathrm{h}} = \sum_{i=1}^{n} [\dot{G}_{\mathrm{h}} C_{\mathrm{p,w}} (T^{i}_{\mathrm{h,in}} - T^{i}_{\mathrm{h,out}})]/n. \tag{2}$$

Then, the SCP and COP are expressed as

$$\mathrm{SCP} = \frac{Q_{\mathrm{ref}}}{m}, \tag{3}$$

$$\mathrm{COP} = \frac{Q_{\mathrm{ref}}}{Q_{\mathrm{h}}}. \tag{4}$$

In the experiments, the flow rates of hot water, cooling water and chilled water are 0.97, 1.4 and 0.44 kg s^{-1} with pressure drops of 4.6, 8.6 and 3.5 mH_2O, respectively. In the experiments, the variations of these values are in a small range.

The accuracy of the flowmeters are 1% FS (full scale), and the full scale is 0~3 m^3 h^{-1} for the chilled water and 3~6 m^3 h^{-1} for the hot water and the cooling water. The maximum deviations of the temperature sensors are ±0.27 °C for the hot water, ±0.21 °C for the cooling water and ±0.19 °C for the chilled water. The accuracy of the timer of the data acquisition system is about 0.55% and the accuracy of the adsorbent mass is 0.1%. According to Eqs. (1) and (4), the maximum relative errors of the cooling capacity and the COP are 7.8% and 1.95%, respectively. The deviation of the SCP is about 7.7% because of the 0.1% accuracy of the electric balance.

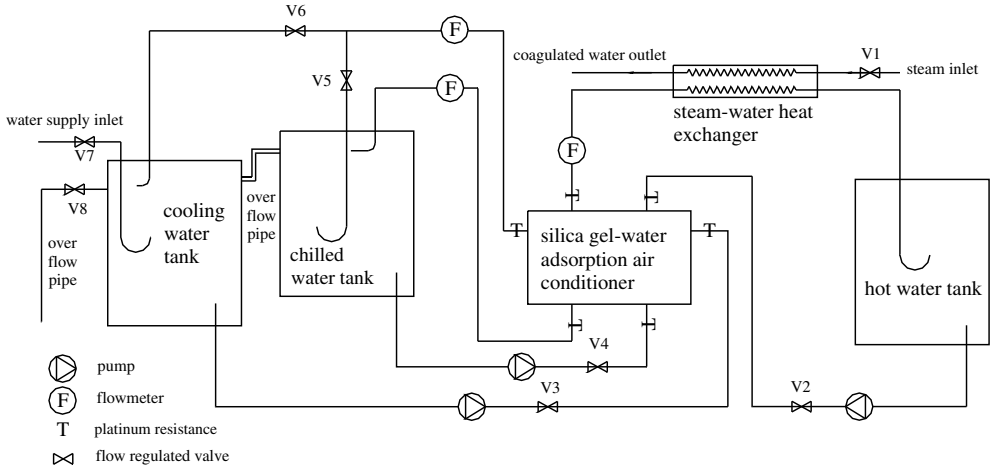

Fig. 5. Experimental system of the silica gel–water adsorption chiller.

4. Results and discussion

4.1. Water temperature variations

Fig. 6 shows the water temperature variations, which are based on the experimental results. The water inlet temperatures of the chiller are fluctuating within a narrow range because the heat accumulation capacity of the water tanks is finite, but the outlet temperatures change in a large range, as well as for the other two bed adsorption systems because the heating/cooling/refrigerating power changes largely in one cycle. During the mass recovery process

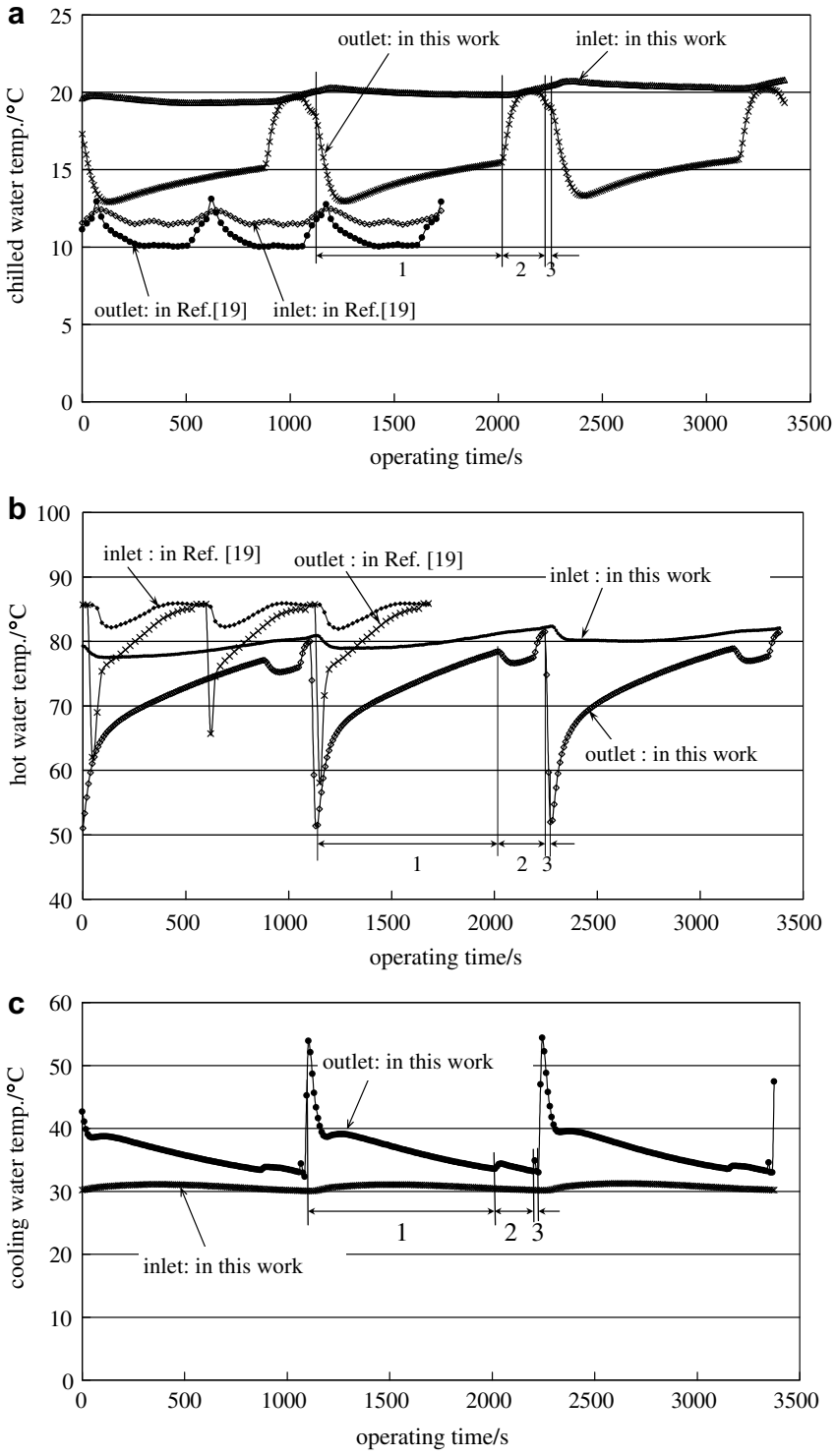

Fig. 6. Temperature variations of the hot water, cooling water and the chilled water (1, heating/cooling phase; 2, mass recovery phase; 3, heat recovery phase) (a) for chilled water, (b) for hot water and (c) for cooling water.

Please cite this article in press as: Xia ZZ et al., Experimental study on improved two-bed ..., Energ Convers Manage (2008), doi:10.1016/j.enconman.2007.12.019

(Phase 2 shown in Fig. 6), the outlet temperature of the hot water drops largely with about 2 °C, for much desorption heat is needed, and the cooling water outlet temperature increases more than 0.5 °C, for much adsorption heat is released. However, these phenomena do not obviously appear in the chiller in [19]. Such large distinctness indicates that the effect of the mass recovery of this chiller is more efficient than that of the former chiller in Ref. [19]. In the heat recovery process (Phase 3 shown in Fig. 6), the temperature of the chilled water will fall, and the refrigeration output yields. In a whole cycle, the chilled water outlet temperature changes from about 13 °C (in adsorption process, Phase 1) to about 20 °C (in mass recovery processes, Phase 3). Compared with the former chiller in [19], the cycle time is almost doubled. The switch frequency of the adsorber is decreased by half, which can prolong the service life of the electric valves, though the low switch frequency indicates that the heat and mass transfer of the adsorber is not good enough. This also shows a potential improvement of this chiller.

4.2. Mass recovery effects

The time without refrigeration output for this chiller in one cycle is much longer than that of the former chiller [19]. So, the length of the mass recovery time must have a different influence on this chiller. The effects of mass recovery time on the chiller are shown in Figs. 7 and 8. Different from the mass recovery like process in [19], the mass recovery process for this improved chiller is quite effective on the refrigerating capacity, with about 65% improvement at the most, as shown in Fig. 8. The mass recovery process sharply increases the cyclic adsorption capacity of the adsorber. So, the mass recovery process greatly improves the performance of the chiller. The mass recovery process increases the refrigerating capacity as well as the heating power. Fur-

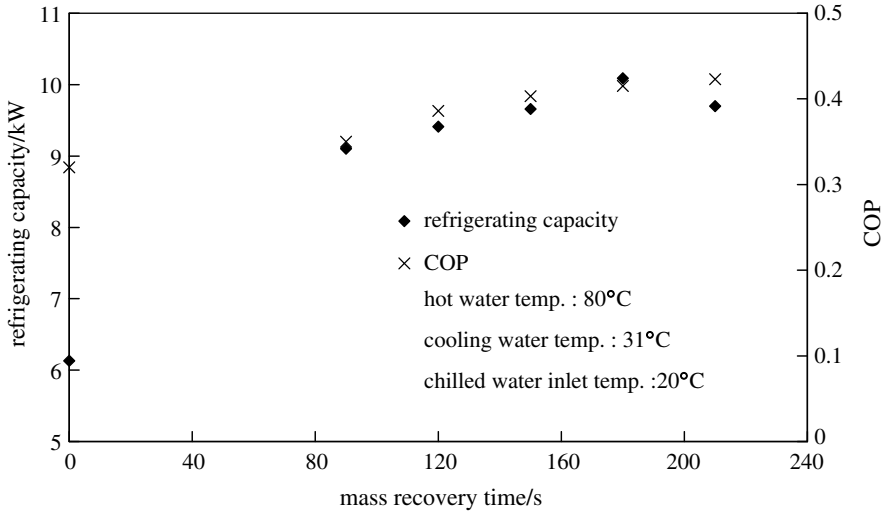

Fig. 7. Refrigerating capacity and COP variations with the mass recovery time.

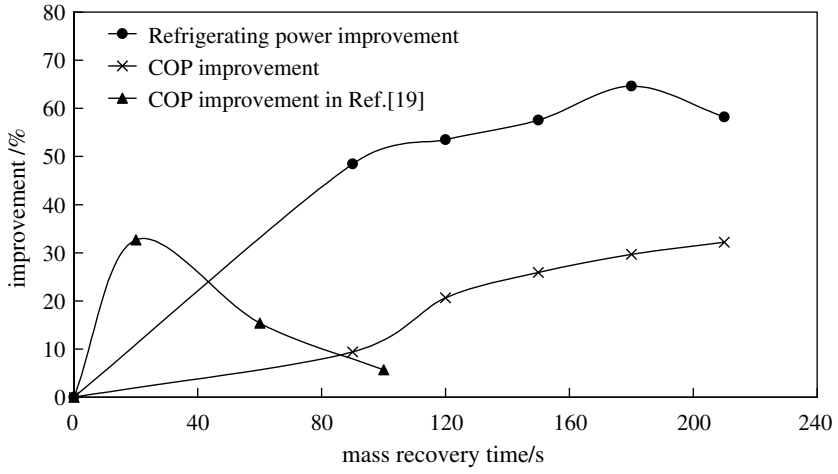

Fig. 8. Improvement of the chiller performance with different mass recovery time.

Please cite this article in press as: Xia ZZ et al., Experimental study on improved two-bed ..., Energ Convers Manage (2008), doi:10.1016/j.enconman.2007.12.019

thermore, the mass recovery time owns a large proportion within one cycle. Therefore, the COP improvement changes slowly with the increase of the mass recovery time and the largest improvement of the COP is only about 32%. Even then, the mass recovery process is more effective to improve the performance of the chiller than that of the former chiller [19]. According to the experimental results, the optimal mass recovery time is about 180 s for the refrigerating capacity and is more than 200 s for the COP, which is many times more than that of the former chiller. As shown in Fig. 7, the COP is also satisfying when the mass recovery time is about 180 s. Therefore, the optimal mass recovery time is about 180 s for a good COP and the best refrigerating capacity.

Figs. 9 and 10 show the performance of the chiller with and without the mass recovery process. Compared with the working condition without the mass recovery process, the mass recovery has improved the refrigerating capacity by 3–4 kW, that is, about 40% of the designed refrigerating capacity of the chiller. However, the effects of the mass recovery on the COP are small because the mass recovery increases the heating power of the chiller as well as the refrigerating capacity. Therefore, it further proves that the mass recovery is crucial to improvement of the refrigerating capacity of the chiller but not to that of the COP.

In the mass recovery process, the adsorber adsorbs water vapor not only from the desorber but also from the Water Evaporator in the desorption side because of the higher saturation vapor pressure in the desorption chamber. During the mass recovery process, the water in the Water Evaporator in the desorption chamber starts evaporating under the adsorption of the adsorber in the other chamber so that the temperature of this water evaporator drops. The temperature of the other water evaporator will rise because its temperature is much lower than both the temperature of the condenser in the same chamber and that of the water evaporator in the desorption chamber, and then, the vapor condenses in this water evapora-

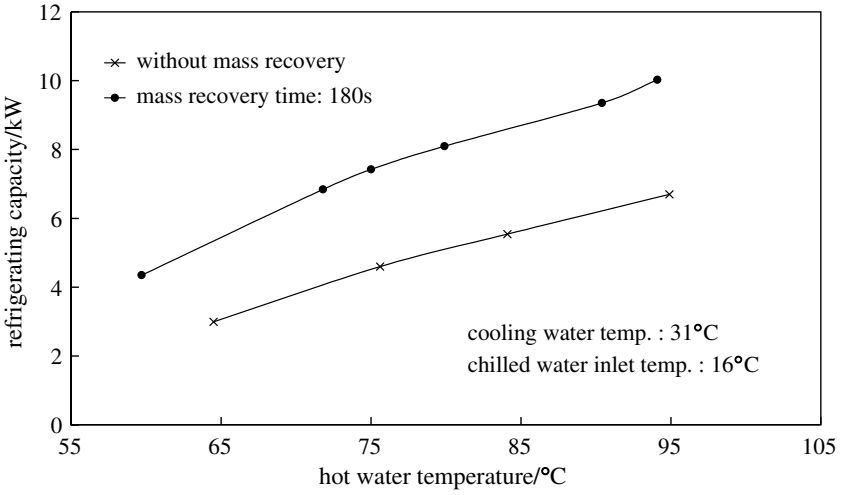

Fig. 9. Effects of the mass recovery on the refrigerating capacity with different hot water temperature.

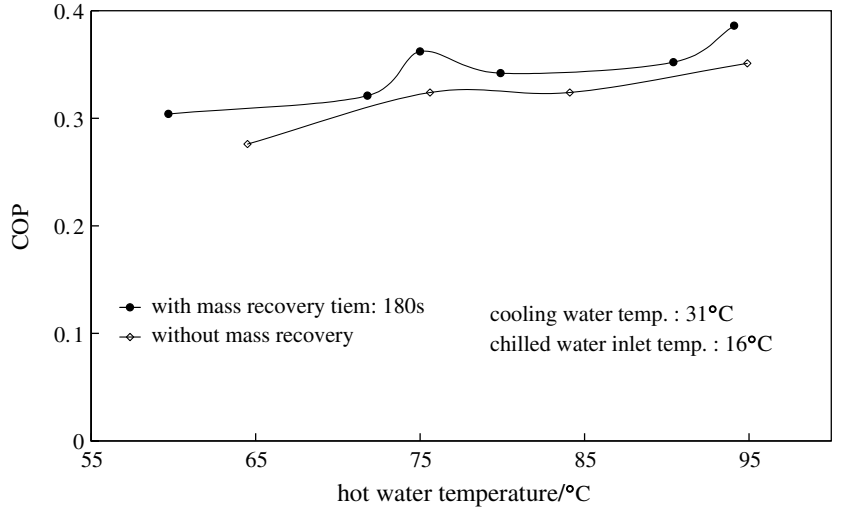

Fig. 10. Effects of the mass recovery on COP with different hot water temperature.

Please cite this article in press as: Xia ZZ et al., Experimental study on improved two-bed ..., Energ Convers Manage (2008), doi:10.1016/j.enconman.2007.12.019

tor. It seems that the refrigeration output from the evaporator in the adsorption chamber is recovered. Therefore, the mass recovery not only increases the cyclic adsorption capacity but also helps the water evaporators exchange heat between each other.

4.3. Performance improvement

Table 1 shows the performance comparisons of the chiller and the former chillers, on the basis of the experimental results. The results given by [19] are mostly on the basis of the cooling water temperature at 28 °C, so only the results near those cases of the test in this work are provided in Table 1.

The refrigerating capacity of the chiller is up to 10.88 kW with the SCP of 104.6 W kg^{-1} under the condition of the cooling water temperature at 30.5 °C, the hot water temperature at 84.4 °C and the chilled water outlet temperature at 16.5 °C. Furthermore, the refrigerating capacity is 4.8 kW if the hot water temperature is about 60 °C and the cooling water temperature is 30.4 °C, though the chilled water outlet temperature is a bit high at 18.2 °C. However, this result indicates that the chiller is very suitable for a low grade heat source, and when the chilled water outlet temperature is 11.8 °C, 8.6 kW of refrigerating capacity is yielded, and the COP is 0.383. Correspondingly, the improvement of performance will be near 57% for SCP and 80.7% for COP at most, compared to the first prototype of the former chiller, even though the hot water temperature in this study is 1.2 °C lower than that of the typical case in [19]. Compared to the second prototype of the former chiller, the most improvement is about 22% for the COP. For a close working condition with the chilled water outlet temperature at about 12 °C, the most improvement of the SCP of this chiller is more than 90%, which is about 83 W kg^{-1}.

Furthermore, the experimental results of the improved chiller in this work are almost consistent with the computational results given by Akahira et al. [17] and at least 12% higher than those in [20] for COP. So, the improvement achieved in the present work for a silica gel–water adsorption chiller can be confirmed.

4.4. Effects of the improvement in the structure of the evaporator

In this work, in order to enhance the heat transfer between the water evaporator and the methanol evaporator, a large area of the surface of the water evaporators exposed to the methanol vapor is needed but causes much methanol attachment to this surface during the evaporating process of this water evaporator. Moreover, some liquid methanol will remain in the bottom of the pipes of the water evaporator because these pipes are arranged horizontally. Therefore, much liquid methanol residue will remain in the walls and pipes of the water evaporator, such as Evaporator 1 before Evaporator 1 is switched into idle. After switchover, the temperature of Evaporator 1 will rise because the water condensation process will occur in Evaporator 1 in the beginning of the desorption/condensation process due to much lower temperature than the temperature of Condenser 1 at this time. Meanwhile, the water evaporation process occurs in Evaporator 2. As a result, the temperature of Evaporator 1 is higher than that of Evaporator 2 or the methanol evaporator. Then, the residual methanol will evaporate from the surface of

Table 1
Experimental results comparisons between the improved chiller and the former chillers

Prototype	Hot water temp. (°C)	Cooling water temp. (°C)	Chilled water temp. (°C)		Refrigerating power (kW)	COP	SCP (W kg^{-1})	Cycle time (s)
			Inlet	Outlet				
The improved chiller	78.8	31.3	20.5	16	8.32	0.31	80	1680
	81.8	31.3	20.7	16.3	9.33	0.34	89.7	1920
	86.8	30.9	21.1	16.3	10.62	0.398	102.1	1920
	59.7	30.4	20.5	18.2	4.80	0.385	46.2	
	69.1	30.3	19.6	16.2	7.57	0.378	72.8	
	84.4	30.5	21.5	16.5	10.88	0.432	104.6	
	85.3	30.6	20.9	16.1	10.44	0.404	100.4	2280
	80.3	30.2	15.8	12.1	8.26	0.382	79.4	
	82.5	30.4	15.8	11.9	8.69	0.388	83.6	
	83.8	30.8	15.4	11.8	8.6	0.383	82.7	
The former chiller in [19]	85	32	14	–	–	0.313[a]	–	1000
	85	30	14	–	–	0.361[a]	–	
	85	32	14	13	2.27	0.188[b]	43	
	85	30	14	12.8	2.79	0.212[b]	52.8	
The chiller in [17]	80	30	14	–	8.6	0.39	–	1140
The chiller in [20]	85	32	14	–	–	0.28	–	–
	85	30	14	–	–	0.34	–	–

[a] On the base of the *second prototype* termed in [19].
[b] On the base of the *first prototype* termed in [19].

Please cite this article in press as: Xia ZZ et al., Experimental study on improved two-bed ..., Energ Convers Manage (2008), doi:10.1016/j.enconman.2007.12.019

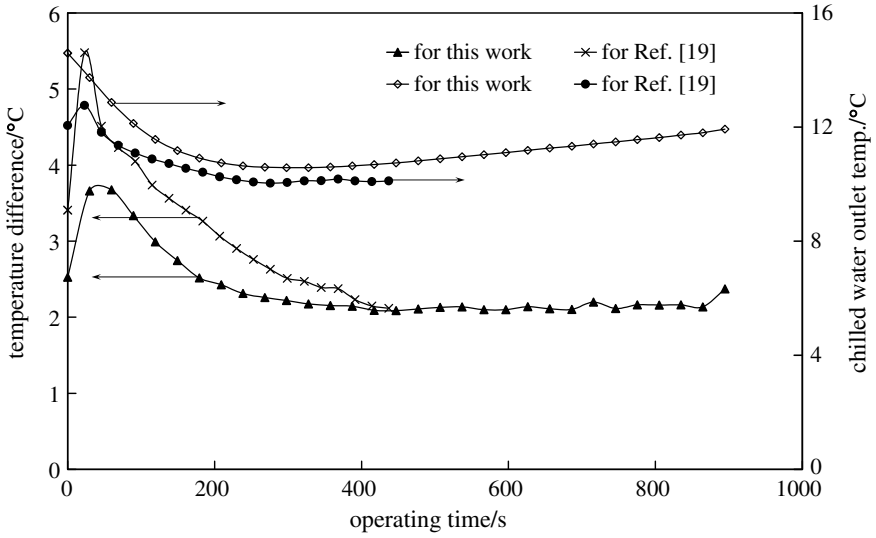

Fig. 11. Comparisons of the temperature difference between the chilled water outlet and the evaporating temperature and of the chilled water outlet temperatures.

Evaporator 1 and condense in Evaporator 2 or the Methanol Evaporator. Consequently, more or less refrigerating capacity loss from the evaporator occurs. This loss can be evaluated in terms of the mass of the evaporator metal and the residual methanol.

$$Q_{\text{loss,improved}} = \frac{m_{\text{we}}C_{\text{cu}}\Delta T_{\text{we}} + L_{\text{meth}}m_{\text{meth,residual}}}{\tau_{\text{cycle}}/2} \approx \frac{65\times 0.386\times 20 + 1250\times 0.453}{2280/2} \approx 0.94\ \text{kW}, \quad (5)$$

$$m_{\text{meth,residual}} \approx \frac{m_{\text{we}}C_{\text{cu}}\Delta T_{\text{we}} + m_{\text{me}}C_{\text{cu}}\Delta T_{\text{me}}}{L} \approx \frac{65\times 0.386\times 20 + 28\times 0.386\times 6}{1250} \approx 0.453\ \text{kg}, \quad (6)$$

where the mass of the residual methanol, $m_{\text{meth,residual}}$, is determined by the physical property of the methanol, the structure of the water evaporator, the surface behavior of the water evaporator and the temperatures of the methanol and the evaporator. So, it is difficult to calculate an accurate value for $m_{\text{meth,residual}}$. A conservative value is estimated on the basis of the temperature drop of the water evaporator and the temperature lift of the methanol evaporator obtained from the experimental results, as expressed by Eq. (6). The temperature difference of the evaporator, ΔT_{e}, is based on the evaporator temperature changing from 35 °C in the end of the desorption/condensation process to 15 °C in the end of the adsorption/evaporation process.

As to the evaporator of the former chiller [19], the refrigeration capacity loss is mainly determined by the heat capacity of the evaporator metal and the heat capacity of the chilled water residual in the evaporator. It can be estimated by the following formula:

$$Q_{\text{loss,former}} = \frac{(M_{\text{e}}C_{\text{cu}} + M_{\text{chilledwater}}C_{\text{p,w}})\Delta T_{\text{e}}}{\tau_{\text{cycle}}/2} = \frac{(32\times 0.386 + 15\times 4.186)\times 20}{1000/2} = 3.01\ \text{kW}. \quad (7)$$

According to the evaluation above, the improvement in the structure of the evaporator is more effective than that of [19]. The refrigerating capacity loss from the evaporator is about 60% of the designed refrigerating capacity for the former chiller, but it is only 9.4% for the improved chiller in this work.

In addition, the variations of the evaporator temperature also indicate that the evaporator of the improved chiller is more effective. The time averaged difference between the evaporator temperature and the chilled water outlet temperature is 2.4 °C in the evaporation process, which is about 0.7 °C lower than that in [19], as shown in Fig. 11. This smaller difference means an improvement in the potential refrigerating capacity of the chiller. The comparisons of the temperature difference between the chilled water outlet and the evaporating temperature during evaporation process in one half cycles are shown in Fig. 11.

5. Conclusions

The improved adsorption chiller with three vacuum chambers in this work is more reliable and suitable. The vacuum valve installed for the mass recovery process makes this chiller more efficient than the chiller with a mass recovery like process. Through the experimental tests, much improvement is achieved in this work and is confirmed as follows:

Please cite this article in press as: Xia ZZ et al., Experimental study on improved two-bed ..., Energ Convers Manage (2008), doi:10.1016/j.enconman.2007.12.019

1) The refrigerating capacity and COP of the chiller are, respectively, 8.69 kW and 0.388 for a heat source at 82.5 °C, the cooling water temperature at 30.4°C and the chilled water outlet temperature at 11.9 °C.
2) If the dehumidification requirement for the chiller is unnecessary, for a chilled water outlet temperature of about 16 °C, the COP reaches 0.432 while the refrigerating capacity is near 11 kW. There is an improvement of at least 12% for the COP compared with the former chillers.
3) The mass recovery process for the chiller causes the most improvement of the refrigerating capacity with about 65% and that of the COP with about 32%. The mass recovery process has a larger influence on the refrigerating capacity, which is quite different from the mass recovery like effects.
4) The evaporator of this improved adsorption chiller is simpler, more efficient and more reliable compared with that of the former chillers [19].

Acknowledgements

This work is supported by the national 863 Program (Hi-tech Research and Development Program of China) under the contract No. 2006AA05Z413 and the Research Award Fund for Young Scientist of Shandong Province under the contract No. 2006BSB01254. We are thankful to the engineers of Jiangsu Shuangliang Air-conditioning Equipment Co. for their help in carrying out the lab investigation.

References

[1] Shelton SV, Wepfer WJ, Miles DJ. Ramp wave analysis of the solid/vapor heat pump. J Energy Resour Technol Trans ASME 1990;112(1):69–78.
[2] Critoph RE. Forced convection enhancement of adsorption cycles. Heat Recovery Syst & CHP 14 1994;16(5):343–50.
[3] Pons M, Szarzynski S. An adsorption cooling system with heat-regeneration: experiment and numerical study. In: Proceedings of the international sorption heat pump conference, Munich, Germany, March 24–26; 1999. p. 625–30.
[4] Sward BK, LeVan D, Meunier F. Adsorption heat pump modeling: the thermal wave process with local equilibrium. Appl Therm Eng 2000;20:759–80.
[5] Critoph RE. Forced convection adsorption cycle with packed bed heat regeneration. Int J Refrig 1999;22(1):38–46.
[6] Critoph RE. Forced convection adsorption cycles. Appl Therm Eng 1998;18:799–807.
[7] Wang RZ. Performance improvement of adsorption heat pump by heat and mass recovery operation. Int J Refrig 2001;24(7):602–11.
[8] Saha BB, Koyama S, Lee JB, Kumahara K, Alam KCA, et al. Performance evaluation of a low-temperature waste heat driven multi-bed adsorption chiller. Int J Multiphase Flow 2003;29(8):1249–63.
[9] Saha BB, Koyama S, Kashiwagi T, Akisawa A, Ng KC, Chua HT. Waste heat driven dual-mode, multi-stage, multi-bed regenerative adsorption system. Int J Refrig 2003;26(7):749–57.
[10] Tai-Hee Eun, Hyun-Kon Song, Jong Hun Han, Kun-Hong Lee, Jong-Nam Kim. Enhancement of heat and mass transfer in silica-expanded graphite composite blocks for adsorption heat pumps: part I. Characterization of the composite blocks. Int J Refrig 2000;23:64–73.
[11] Tai-Hee Eun, Hyun-Kon Song, Jong Hun Han, Kun-Hong Lee, Jong-Nam Kim. Enhancement of heat and mass transfer in silica-expanded graphite composite blocks for adsorption heat pumps: part II. Cooling system using the composite blocks. Int J Refrig 2000;23:74–81.
[12] Miltkau T, Dawoud B. Dynamic modeling of the combined heat and mass transfer during the adsorption/desorption of water vapor into/from a zeolite layer of an adsorption heat pump. Int J Therm Sci 2002;41:753–62.
[13] Tatlıer M, Tantekin-Ersolmaz B, Erdem-Senatalar A. A novel approach to enhance heat and mass transfer in adsorption heat pumps using the zeolite–water pair. Microporous Mesoporous Mater 1999;27:1–10.
[14] Saha BB, Boelman EC, Kashiwagi T. Computational analysis of an advanced adsorption–refrigeration cycle. Energy 1995;20:983–94.
[15] Hamamoto Y, Akisawa A, Haga N, Kashiwagi T. Experimental study on two-stage adsorption refrigeration system. In: Proceedings of the international sorption heat pump conference, Shanghai, China, 2002. p. 550–55.
[16] Chua HT, Ng KC, Malek A, Kashiwagi T, Akisawa A, Saha BB. Multi-bed regenerative adsorption chiller-improving the utilization of waste heat and reducing the chilled water outlet temperature fluctuation. Int J Refrig 2001;24:124–36.
[17] Akahira A, Alam KCA, Hamamoto Y, Akisawa A, Kashiwagi T. Mass recovery adsorption refrigeration cycle-improving cooling capacity. Int J Refrig 2004;27:225–34.
[18] Chua HT, Ng KC, Malek A, et al. Modeling the performance of two-bed, silica gel–water adsorption chillers. Int J Refrig 1999;22:194–204.
[19] Liu YL, Wang RZ, Xia ZZ. Experimental study on a continuous adsorption water chiller with novel design. J Refrig 2005;28(2):218–30.
[20] Saha BB, Boelman EC, Kashiwagi T. Computer simulation of a silica gel–water adsorption refrigeration cycle the influence of operating conditions on cooling output and COP. ASHRAE Trans Res 1995;101(2):348–55.
[21] Wang DC, Wu JY, Xia ZZ, et al. Study of a novel silica gel-water adsorption chiller: part I. Design and performance prediction. Int J Refrig 2005;28(7):1073–83.